PROCEEDINGS OF SCIENCE

ICRC 2021 THE ASTROPARTICLE PHYSICS CONFERENCE Berlin | Germany
37th International Cosmic Ray Conference 12–23 July 2021

Neutrino non-standard interactions with the KM3NeT/ORCA detector

Jerzy Mańczak[a,*], **Nafis Rezwan Khan Chowdhury**[a,1], **Juan José Hernández-Rey**[a] **and Sergio Navas Concha**[b] **on behalf of the KM3NeT Collaboration**
(a complete list of authors can be found at the end of the proceedings)

[a] *Instituto de Fisica Corpuscular (University of Valencia and CSIC), Calle Jose Beltran 2, Paterna, Spain*
[b] *Univesidad de Granada, Avda. del Hospicio, s/n C.P. 18010 Granada, Spain*
E-mail: jmanczak@ific.uv.es, nafis.chowdhury@ific.uv.es, juanjo@ific.uv.es, navas@ugr.es

KM3NeT/ORCA is a dense array that constitutes the low-energy branch of the KM3NeT project with the main goal of resolving the question of the neutrino mass ordering. At present, the KM3NeT/ORCA Phase 1 has already been deployed, which means that six out of the planned 115 detection lines are operational. Even with this limited configuration, neutrino oscillations can already be measured and studied. In this contribution, the sensitivity to the neutrino Non-Standard Interactions (NSI) parameter $\epsilon_{\mu\tau}$ using the current stage of the KM3NeT/ORCA detector together with the projections for the final configuration are presented.

37th International Cosmic Ray Conference (ICRC 2021)
July 12th – 23rd, 2021
Online – Berlin, Germany

[1] now at University of Utah , Dept. of Physics and Astronomy, Salt Lake City, USA
[*] Presenter

PoS(ICRC2021)1165

1. Introduction

Neutrino Non-Standard Interactions (NSI) are one of the possible sub-dominant effects which can affect neutrinos propagating through matter via observable changes in the oscillation patterns predicted by "standard" oscillations. These NSI can modify the neutrino flavour ratios observed in neutrino telescopes that measure the atmospheric neutrino flux. Experiments such as ANTARES [1] and IceCube [2] have already proven their capability to measure NSI parameters with particularly sensitive prospects in the μ–τ sector. Due to the limited size of KM3NeT/ORCA6, in this contribution we focus exclusively on $\epsilon_{\mu\tau}$.

2. Non-Standard Interactions

NSI interactions are customarily defined as those subset of interactions beyond the Standard Model whose currents involve chirally left neutrinos and left and right charged fermions. Neutrino propagation through the Earth's matter in the presence of neutral current NSI can be described by the following effective Hamiltonian [3]:

$$H_{eff} = \frac{1}{2E} U_{PMNS} \begin{bmatrix} 0 & 0 & 0 \\ 0 & \Delta m^2_{21} & 0 \\ 0 & 0 & \Delta m^2_{31} \end{bmatrix} U^{\dagger}_{PMNS} + V_{CC} \begin{bmatrix} 1+\epsilon_{ee} & \epsilon_{e\mu} & \epsilon_{e\tau} \\ \epsilon^*_{e\mu} & \epsilon_{\mu\mu} & \epsilon_{\mu\tau} \\ \epsilon^*_{e\tau} & \epsilon^*_{\mu\tau} & \epsilon_{\tau\tau} \end{bmatrix}, \tag{1}$$

where $V_{CC} = \sqrt{2} G_F n_e$ is the electron Earth matter potential associated with the MSW effect [4] and the NSI parameters $\epsilon_{\alpha\beta}$ (with $\alpha, \beta = (e, \mu, \tau)$) can be expressed as

$$\epsilon_{\alpha\beta} = \epsilon^{eC}_{\alpha\beta} + \frac{n_u}{n_e}\epsilon^{uC}_{\alpha\beta} + \frac{n_d}{n_e}\epsilon^{dC}_{\alpha\beta},$$

in terms of their coupling strength ϵ^{fC} to different fermions ($f = e, u, d$). For simplicity, the interactions with u quarks and electrons are neglected so that in this contribution we assume a uniform Earth density profile with a relation $n_d = 3n_e$, a given NSI parameter $\epsilon_{\mu\tau} = 3\epsilon^{dC}_{\alpha\beta}$. The results presented here can be re-scaled to obtain the NSI coupling strengths to the other fermions. Generally the NSI parameters can carry a complex phase, but in this study only their real part is considered. Figure 1 shows the effect of opposite values of $\epsilon_{\mu\tau}$ in comparison to standard oscillations for the muon neutrinos. As can be seen, neutrino energies higher than 100 GeV can be relevant for $\epsilon_{\mu\tau}$, whereas the standard atmospheric neutrino oscillations are normally probed with energies up to 50 GeV. This feature gives an opportunity also for telescopes optimized for higher neutrino energies to measure this particular NSI parameter.

3. KM3NeT/ORCA detector

ORCA (Oscillations Research with Cosmics in the Abyss) is the low-energy node of KM3NeT, the next generation underwater neutrino detector in the Mediterranean sea. The final KM3NeT/ORCA detector block will consist of 115 DUs (Detection Units or "strings") densely placed in a circle on the seabed with a horizontal grid pitch of around 20m and a vertical length of around 200 m. Each

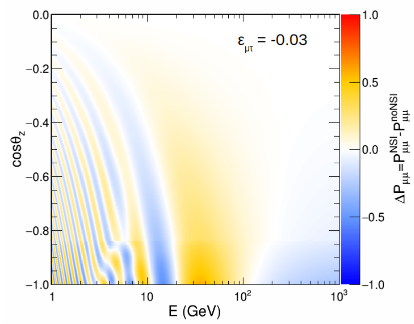

(a) Survival probability difference between standard oscillations NuFit [5] best fit values (NoNSI) and $\epsilon_{\mu\tau} = -0.03$ (NSI) for summed $\nu_\mu + \bar{\nu}_\mu$

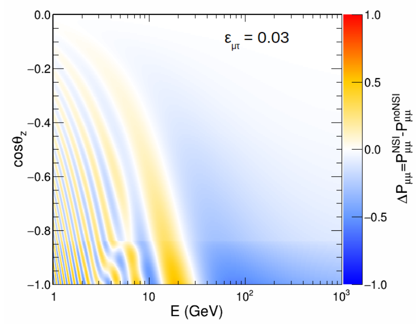

(b) Survival probability difference between standard oscillations NuFit [5] best fit values and $\epsilon_{\mu\tau} = 0.03$ (NSI) for summed $\nu_\mu + \bar{\nu}_\mu$

Figure 1: Impact of $\epsilon_{\mu\tau}$ on ν_μ oscillations

DU comprises 18 DOMs (Digital-Optical Modules) each equipped with 31 3-inch photomultipliers (PMTs) and sensitive to the Cerenkov light induced by the charged products of the neutrino interactions with the seawater. The vertical distance between DOMs is 9 meters. The present configuration of ORCA has six DUs deployed and operating. The primary goal of KM3NeT/ORCA is the determination of the neutrino mass ordering [6]. With an energy threshold of a few GeV and an effective mass of several Mtons, KM3NeT/ORCA can also make precision measurements of atmospheric neutrino oscillation parameters. Moreover, its access to a wide range of energies and baselines makes it optimal to discover exotic physics beyond the Standard Model such as NSI. Already with a few DUs, KM3NeT/ORCA proves to be capable of probing neutrino oscillation effects [7]. In the following sections, the KM3NeT/ORCA full detector block with 115 DUs is referred to as ORCA115 and the current detector configuration of KM3NeT/ORCA Phase1 with six operational lines is abbreviated as ORCA6.

4. Monte Carlo sample and event selection

Two event topologies can be distinguished in KM3NeT/ORCA: track-like and shower-like events. Tracks are mostly produced by the CC interactions of muon neutrinos and the majority of showers are caused by all-flavour NC interactions and CC interactions of electron neutrinos. However, the detector event rate is dominated by atmospheric muons. For this reason, a strong muon background suppression method has to be applied. A cut on incoming zenith angle allowing only events arriving to the detector from below ("up-going"), greatly reduces the atmospheric muon background, while still leaving atmospheric neutrinos in a wide range of zenith angles and thus baselines, which is necessary for any oscillation analysis. The MC sample is generated using a staged approach in which gSeagen [8] is responsible for the neutrino event generation, MUPAGE [9] is used for the muon generation and all the events are then propagated and triggered with the internal KM3NeT software Jpp [6]. Finally, the track and shower reconstruction stage is taken care of by separate algorithms.

PoS(ICRC2021)1165

4.1 ORCA115

For ORCA115 machine-learning RDF-based algorithms (Random Decision Forest) were developed for the particle identification (PID) and background suppression. Using the PID track score, the sample gets divided into three classes representing tracks, showers and intermediates (events with ambiguous topology). Atmospheric muon contamination and other sources of background noise are very efficiently excluded from the sample with dedicated machine-learning algorithms [10].

4.1.1 Systematic uncertainties

The set of systematic parameters used for the NSI analysis with ORCA115 can be seen in the table of Fig. 2, right, and their cumulative impact in the plot of Fig. 2, left. The systematic uncertainties with the strongest impact on the NSI study with ORCA115 come from the unconstrained standard oscillation parameters.

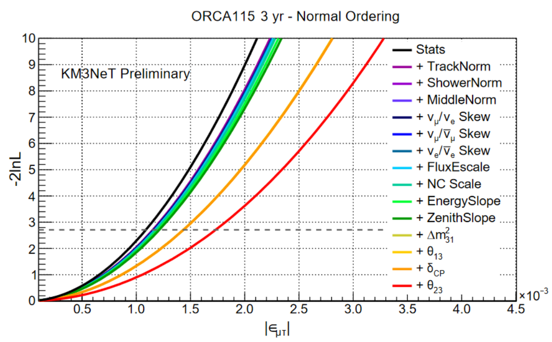

(a) Incremental impact on $\epsilon_{\mu\tau}$ sensitivity of all the systematic parameters used for ORCA115.

Nuisance parameters	Treatment	Nominal values	Priors
Oscillation			
$\theta_{12}(^\circ)$	fixed	33.82	-
$\theta_{13}(^\circ)$	fitted	8.60	0.13
$\theta_{23}(^\circ)$	fitted	48.6	free
$\delta_{CP}(^\circ)$	fitted	221	free
$\Delta m^2_{21}(\times 10^{-5}\mathrm{eV}^2)$	fixed	7.39	-
$\Delta m^2_{31}(\times 10^{-3}\mathrm{eV}^2)$	fitted	2.528	free
Flux			
Track norm.	fitted	1	free
Shower norm.	fitted	1	free
Middle norm.	fitted	1	free
ν_μ/ν_e skew	fitted	0	5%
$\nu_\mu/\bar{\nu}_\mu$ skew	fitted	0	5%
$\nu_e/\bar{\nu}_e$ skew	fitted	0	5%
Energy slope ($\Delta\gamma$)	fitted	0	5%
Zenith slope	fitted	0	2%
Cross-section			
NC scale	fitted	1	5%
Detector			
Energy scale	fitted	1	10%

(b) Table of systematic parameters used with ORCA115 [1].

Figure 2: Systematics with ORCA115 sample

4.2 ORCA6

Shower reconstruction is still not optimised for the limited size of ORCA6, so that only track reconstruction is taken into account in this study. For this reason, even without PID, the fraction of ν_μ in the ORCA6 MC reconstructed neutrino sample reaches roughly 70%. As a proxy of the deposited energy a simplified approach is applied where the reconstructed track length divided by 4 is used to approximate the energy of minimum ionizing muons in water for which $dE/dx \simeq 0.25\,\mathrm{GeV/m}$. This method naturally introduces a cut on the maximum reconstructed energy $E^{max}_{reco} \simeq 50\,\mathrm{GeV}$ driven by the detector size. The distributions of energy and angular resolutions obtained are shown in Fig 3, where the saturation effect on the reconstructed energy is clearly visible.

Figure 4 shows the event distribution obtained for ORCA6 with an oscillated, 1-year equivalent Monte Carlo simulated sample, in the true L/E (oscillation length divided by energy) space, after the selection is applied. Despite all the limitations mentioned above, ORCA6 is capable of observing the effect of $\epsilon_{\mu\tau}$ on neutrino oscillations at a significant level.

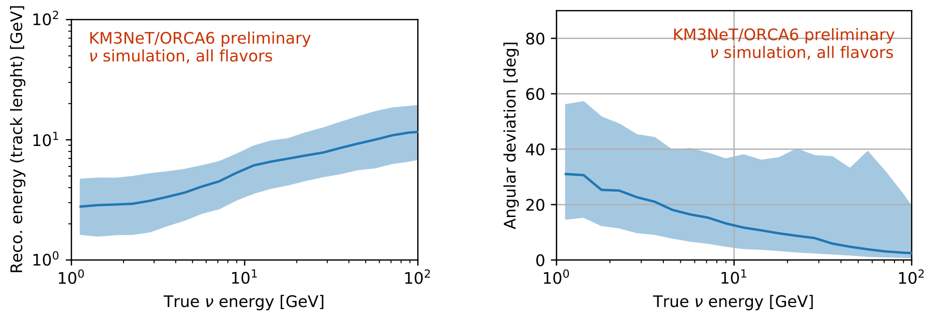

(a) Resolution of the reconstructed energy. **(b)** Resolution of the reconstructed direction.

Figure 3: Resolution of the reconstructed energy and arrival direction as a function of the true neutrino energy for ORCA6.

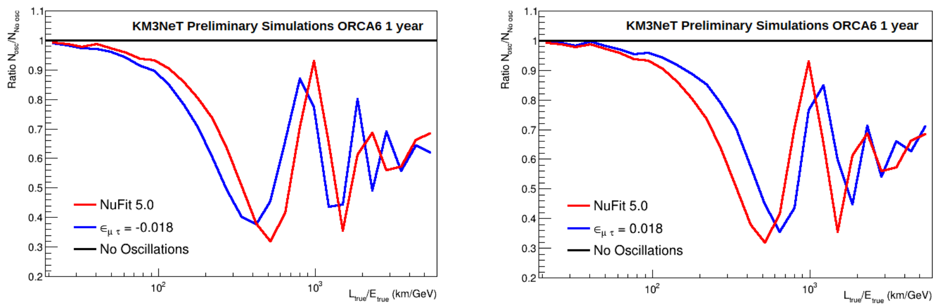

(a) Oscillated event rates ratios to unoscillated sample for standard oscillation best fit parameters and the set extended by $\epsilon_{\mu\tau} = -0.018$.

(b) Oscillated event rates ratios to unoscillated sample for standard oscillation best fit parameters and the set extended by $\epsilon_{\mu\tau} = 0.018$.

Figure 4: One-year ORCA6 distributions of the ratio of event rates for oscillated to unoscillated MC as a function of the true oscillation length divided by the true neutrino energy for the selected events.

4.2.1 Systematic uncertainties

The impact of the systematic uncertainties in the ORCA6 sample for the NSI study is still being investigated. So far it was found that the nuisance parameter with the largest influence is Δm^2_{31}. Figure 5 shows the ORCA6 90% CL sensitivity allowed regions in 2D space spanned by Δm^2_{31} and $\epsilon_{\mu\tau}$. Despite a mild correlation, for the current detector exposure of approximately one year, ORCA6 sensitivity is expected to be dominated by the sample statistics.

5. Analysis method

All the KM3NeT/ORCA median sensitivities presented in this contribution are based on the Asimov data set approach and Wilk's theorem.

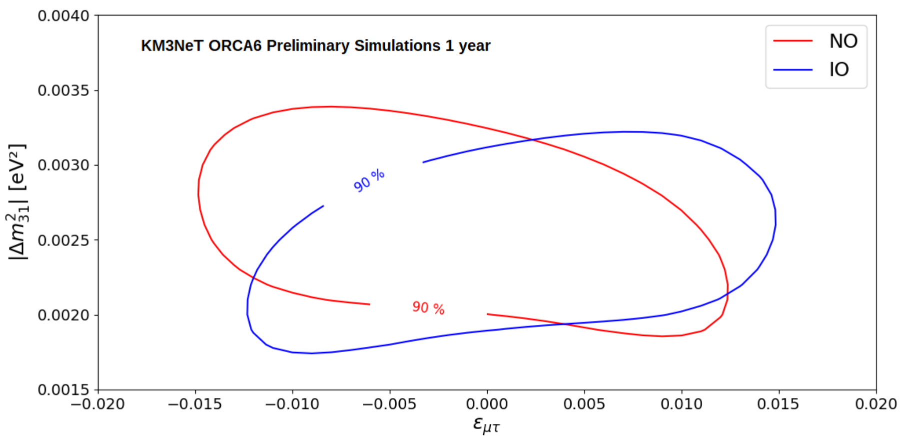

Figure 5: 90% CL sensitivity contours in $\epsilon_{\mu\tau}$ and Δm^2_{31} with ORCA6 1 year MC sample for both mass hierarchies assuming true NO.

5.1 ORCA115

To study the ORCA115 sensitivity, a profile Poisson likelihood ratio is calculated with respect to the non-NSI pseudo-data nominal parameters:

$$-2\ln\left(\frac{L(\epsilon_{\mu\tau},\eta)}{L(0,\hat{\hat{\eta}})}\right) = 2\sum_{bins}\left(N_{NSI}(\epsilon_{\mu\tau},\eta) - N_{STD}(0,\hat{\hat{\eta}}) + N_{STD}(0,\hat{\hat{\eta}})\ln\frac{N_{STD}(0,\hat{\hat{\eta}})}{N_{NSI}(\epsilon_{\mu\tau},\eta)}\right) + \sum_{syst}\frac{\eta-\bar{\eta}}{2\sigma^2_{\eta}}, \tag{2}$$

where $\hat{\hat{\eta}}$ here indicates the nominal values of the nuisance parameters. For each point scanned in $\epsilon_{\mu\tau}$, the sum of the likelihood ratio (Eq. 2) from all the separate PID classes (see section 4.1) is minimized over the set of the nuisance parameters $\{\eta\}$. The second term corresponds to the external gaussian constraints on the nuisance parameters (both from the physics and the experimental systematics) with mean $\bar{\eta}$ at their nominal values of pseudo-data and standard deviation σ_η described as prior in the table of Fig 2.

5.2 ORCA6

As mentioned in section 4.2.1, the systematic uncertainties have not been fully investigated yet for ORCA6, therefore no minimization is performed for the NSI sensitivity study. The pseudo-data set is created for NO (Normal Ordering) with NSI set to zero. For each value of $\epsilon_{\mu\tau}$ the minimum of the negative Poisson likelihood calculated for the NO and IO NuFit[5] standard oscillation parameters is taken, so the profiling is done only over the mass ordering. The Likelihood ratio is then calculated with respect to the generated pseudo-data parameters.

6. KM3NeT/ORCA sensitivity for $\epsilon_{\mu\tau}$

As can be seen in Fig 6 almost all the sensitivity for $\epsilon_{\mu\tau}$ with KM3NeT/ORCA comes from the track events populated mainly by atmospheric $\nu_\mu(\bar{\nu}_\mu)$ oscillating to $\nu_\tau(\bar{\nu}_\tau)$.

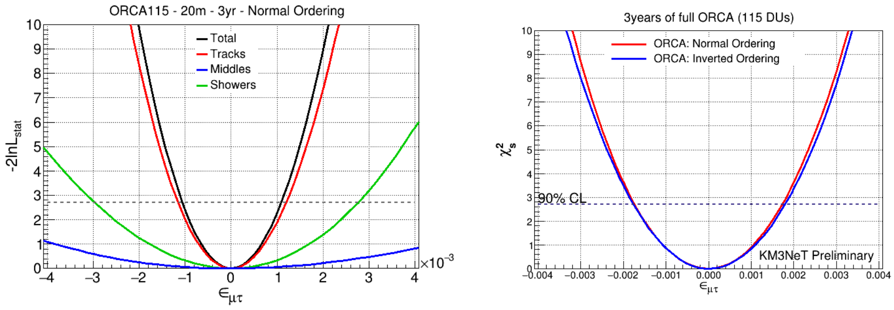

(a) Contributions to ORCA115 sensitivity for $\epsilon_{\mu\tau}$ from different PID classes.

(b) ORCA115 $\epsilon_{\mu\tau}$ sensitivity dependence on the neutrino mass ordering.

Figure 6: Impact on $\epsilon_{\mu\tau}$ sensitivity from different PID with ORCA115 classes and varying mass ordering.

Figure 7 shows the sensitivities of ORCA6 and ORCA115 for $\epsilon_{\mu\tau}$ compared with limits from other experiments. The 90% CL sensitivities assuming NO are:

- for 1 year of ORCA6 (statistics only):

$$-12 \times 10^{-3} < \epsilon_{\mu\tau} < 12 \times 10^{-3},$$

- for 3 years of ORCA115 (full set of systematics):

$$-1.7 \times 10^{-3} < \epsilon_{\mu\tau} < 1.7 \times 10^{-3}.$$

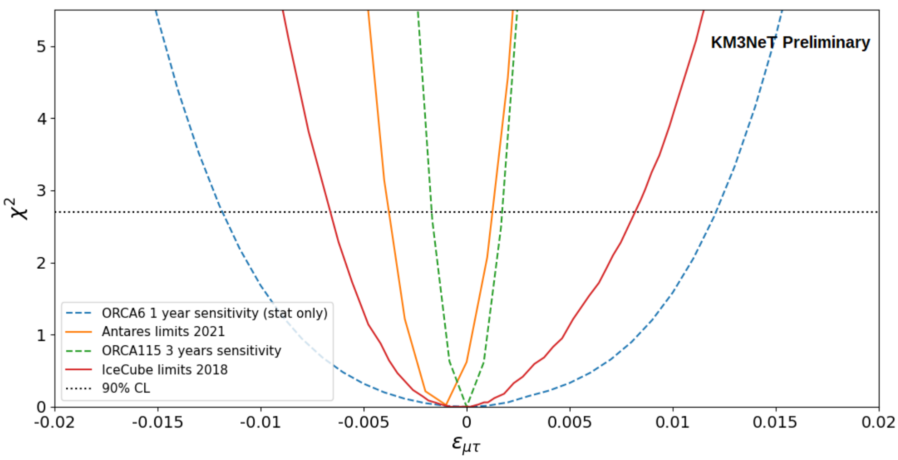

Figure 7: KM3NeT/ORCA sensitivties compared with the best worldwide limits from IceCube[2] and ANTARES[1]

7. Summary

In this work, we have estimated the limits reachable with one year of data-taking of ORCA6 and with three years of the future ORCA115 detector. Using only one year of data-taking, the ORCA6 configuration, which constitutes about 5% of the full detector, is able to reach a measurement precision of $\epsilon_{\mu\tau}$ only two to three times worse than the current limit. Moreover, as ORCA grows in size, not only the event statistics per running time will increase, but also the energy resolution and the highest measurable muon energy, which will improve significantly the sensitivity to the $\epsilon_{\mu\tau}$ parameter. When completed, the KM3NeT/ORCA detector will potentially become the world's best tool for probing neutrino non-standard interactions with atmospheric neutrinos.

Acknowledgements

This research received support from "la Caixa" Foundation (ID 100010434) through the fellowship LCF/BQ/IN17/11620019, the European Union's Horizon 2020 research and innovation programme under the Marie Skłodowska-Curie grant agreement no. 713673. We gratefully acknowledge as well the financial support of the Ministerio de Ciencia, Innovación y Universidades: Programa Estatal de Generación de Conocmiento, ref. PGC2018-096663-B-C41 (MCIU/ERDF)) and PROMETEO/2020/019 of Generalitat Valenciana.

References

[1] N.R. Khan Chowdhury, *Search for Neutrino Non-Standard Interactions with ANTARES and KM3NeT-ORCA*, Ph.D. thesis, University of Valencia, IFIC, 2021.

[2] IceCube collaboration, *Search for Nonstandard Neutrino Interactions with IceCube DeepCore*, *Phys. Rev. D* **97** (2018) 072009 [1709.07079].

[3] T. Ohlsson, *Status of non-standard neutrino interactions*, *Rept. Prog. Phys.* **76** (2013) 044201 [1209.2710].

[4] L. Wolfenstein, *Neutrino Oscillations in Matter*, *Phys. Rev. D* **17** (1978) 2369.

[5] I. Esteban, M.C. Gonzalez-Garcia, M. Maltoni, T. Schwetz and A. Zhou, *The fate of hints: updated global analysis of three-flavor neutrino oscillations*, *JHEP* **09** (2020) 178 [2007.14792].

[6] KM3NeT collaboration, *Letter of intent for KM3NeT 2.0*, *J. Phys. G* **43** (2016) 084001 [1601.07459].

[7] KM3NeT collaboration, L. Nauta et. al., *First neutrino oscillation measurement with KM3NeT/ORCA*. 345, these Proceedings.

[8] S. Aiello, A. Albert, S.A. Garre, Z. Aly, F. Ameli, M. Andre et al., *gseagen: The km3net genie-based code for neutrino telescopes*, *Computer Physics Communications* **256** (2020) 107477.

[9] G. Carminati, A. Margiotta and M. Spurio, *Atmospheric MUons from PArametric formulas: A Fast GEnerator for neutrino telescopes (MUPAGE)*, *Comput. Phys. Commun.* **179** (2008) 915 [0802.0562].

[10] KM3NeT collaboration, *Determining the Neutrino Mass Ordering and Oscillation Parameters with KM3NeT/ORCA*, 2103.09885.

Full Author List: KM3NeT Collaboration

M. Ageron[1], S. Aiello[2], A. Albert[3,55], M. Alshamsi[4], S. Alves Garre[5], Z. Aly[1], A. Ambrosone[6,7], F. Ameli[8], M. Andre[9], G. Androulakis[10], M. Anghinolfi[11], M. Anguita[12], G. Anton[13], M. Ardid[14], S. Ardid[14], W. Assal[1], J. Aublin[4], C. Bagatelas[10], B. Baret[4], S. Basegmez du Pree[15], M. Bendahman[4,16], F. Benfenati[17,18], E. Berbee[15], A. M. van den Berg[19], V. Bertin[1], S. Beurthey[1], V. van Beveren[15], S. Biagi[20], M. Billault[1], M. Bissinger[13], M. Boettcher[21], M. Bou Cabo[22], J. Boumaaza[16], M. Bouta[23], C. Boutonnet[4], G. Bouvet[24], M. Bouwhuis[15], C. Bozza[25], H.Brânzaş[26], R. Bruijn[15,27], J. Brunner[1], R. Bruno[2], E. Buis[28], R. Buompane[6,29], J. Busto[1], B. Caiffi[11], L. Caillat[1], D. Calvo[5], S. Campion[30,8], A. Capone[30,8], H. Carduner[24], V. Carretero[5], P. Castaldi[17,31], S. Celli[30,8], R. Cereseto[11], M. Chabab[32], C. Champion[4], N. Chau[4], A. Chen[33], S. Cherubini[20,34], V. Chiarella[35], T. Chiarusi[17], M. Circella[36], R. Cocimano[20], J. A. B. Coelho[4], A. Coleiro[4], M. Colomer Molla[4,5], S. Colonges[4], R. Coniglione[20], A. Cosquer[1], P. Coyle[1], M. Cresta[11], A. Creusot[4], A. Cruz[37], G. Cuttone[20], A. D'Amico[15], R. Dallier[24], B. De Martino[1], M. De Palma[36,38], I. Di Palma[30,8], A. F. Díaz[12], D. Diego-Tortosa[14], C. Distefano[20], A. Domi[15,27], C. Donzaud[4], D. Dornic[1], M. Dörr[39], D. Drouhin[3,55], T. Eberl[13], A. Eddyamoui[16], T. van Eeden[15], D. van Eijk[15], I. El Bojaddaini[23], H. Eljarrari[16], D. Elsaesser[39], A. Enzenhöfer[1], V. Espinosa[14], P. Fermani[30,8], G. Ferrara[20,34], M. D. Filipović[40], F. Filippini[17,18], J. Fransen[15], L. A. Fusco[1], D. Gajanana[15], T. Gal[13], J. García Méndez[14], A. Garcia Soto[5], E. Garçon[1], F. Garufi[6,7], C. Gatius[15], N. Geißelbrecht[13], L. Gialanella[6,29], E. Giorgio[20], S.R. Gozzini[5], R. Gracia[15], K. Graf[13], G. Grella[41], D. Guderian[56], C. Guidi[11,42], B. Guillon[43], M. Gutiérrez[44], J. Haefner[13], S. Hallmann[13], H. Hamdaoui[16], H. van Haren[45], A. Heijboer[15], A. Hekalo[39], L. Hennig[13], S. Henry[1], J. J. Hernández-Rey[5], J. Hofestädt[13], F. Huang[1], W. Idrissi Ibnsalih[6,29], A. Ilioni[4], G. Illuminati[17,18,4], C.W. James[37], D. Janezashvili[46], P. Jansweijer[15], M. de Jong[15,47], P. de Jong[15,27], B.J. Jung[15], M. Kadler[39], P. Kalaczyński[48], O. Kalekin[13], U. F. Katz[13], F. Kayzel[15], P. Keller[1], N. R. Khan Chowdhury[5], G. Kistauri[46], F. van der Knaap[28], P. Kooijman[27,57], A. Kouchner[4,49], M. Kreter[21], V. Kulikovskiy[11], M. Labalme[43], P. Lagier[1], R. Lahmann[13], P. Lamare[1], M. Lamoureux[14], G. Larosa[20], C. Lastoria[1], J. Laurence[1], A. Lazo[5], R. Le Breton[4], E. Le Guirriec[1], S. Le Stum[1], G. Lehaut[43], O. Leonardi[20], F. Leone[20,34], E. Leonora[2], C. Lerouvillois[1], J. Lesrel[4], N. Lessing[13], G. Levi[17,18], M. Lincetto[1], M. Lindsey Clark[4], T. Lipreau[24], C. LLorens Alvarez[14], A. Lonardo[8], F. Longhitano[2], D. Lopez-Coto[44], N. Lumb[1], L. Maderer[4], J. Majumdar[15], J. Mańczak[5], A. Margiotta[17,18], A. Marinelli[6], A. Marini[1], C. Markou[10], L. Martin[24], J. A. Martínez-Mora[14], A. Martini[35], F. Marzaioli[6,29], S. Mastroianni[6], K. W. Melis[15], G. Miele[6,7], P. Migliozzi[6], E. Migneco[20], P. Mijakowski[48], L. S. Miranda[50], C. M. Mollo[6], M. Mongelli[36], A. Moussa[23], R. Muller[15], P. Musico[11], M. Musumeci[20], L. Nauta[15], S. Navas[44], C. A. Nicolau[8], B. Nkosi[33], B. Ó Fearraigh[15,27], M. O'Sullivan[37], A. Orlando[20], G. Ottonello[11], S. Ottonello[11], J. Palacios González[5], G. Papalashvili[46], R. Papaleo[20], C. Pastore[36], A. M. Păun[26], G.E. Păvălaş[26], G. Pellegrini[17], C. Pellegrino[18,58], M. Perrin-Terrin[1], V. Pestel[15], P. Piattelli[20], C. Pieterse[5], O. Pisanti[6,7], C. Poirè[14], V. Popa[26], T. Pradier[3], F. Pratolongo[11], I. Probst[13], G. Pühlhofer[51], S. Pulvirenti[20], G. Quéméner[43], N. Randazzo[2], A. Rapicavoli[34], S. Razzaque[50], D. Real[5], S. Reck[13], G. Riccobene[20], L. Rigalleau[24], A. Romanov[11,42], A. Rovelli[20], J. Royon[1], F. Salesa Greus[5], D.F.E. Samtleben[15,47], A. Sánchez Losa[36,5], M. Sanguineti[11,42], A. Santangelo[51], D. Santonocito[20], P. Sapienza[20], J. Schmelling[15], J. Schnabel[13], M. F. Schneider[13], J. Schumann[13], H. M. Schutte[21], J. Seneca[15], I. Sgura[36], R. Shanidze[46], A. Sharma[52], A. Sinopoulou[10], B. Spisso[41,6], M. Spurio[17,18], D. Stavropoulos[10], J. Steijger[15], S.M. Stellacci[41,6], M. Taiuti[11,42], F. Tatone[36], Y. Tayalati[16], E. Tenllado[44], D. Tézier[1], T. Thakore[5], S. Theraube[1], H. Thiersen[21], P. Timmer[15], S. Tingay[37], S. Tsagkli[10], V. Tsourapis[10], E. Tzamariudaki[10], D. Tzanetatos[10], C. Valieri[17], V. Van Elewyck[4,49], G. Vasileiadis[53], F. Versari[17,18], S. Viola[20], D. Vivolo[6,29], G. de Wasseige[4], J. Wilms[54], R. Wojaczyński[48], E. de Wolf[15,27], T. Yousfi[23], S. Zavatarelli[11], A. Zegarelli[30,8], D. Zito[20], J. D. Zornoza[5], J. Zúñiga[5], N. Zywucka[21].

[1]Aix Marseille Univ, CNRS/IN2P3, CPPM, Marseille, France.
[2]INFN, Sezione di Catania, Via Santa Sofia 64, Catania, 95123 Italy.
[3]Université de Strasbourg, CNRS, IPHC UMR 7178, F-67000 Strasbourg, France.
[4]Université de Paris, CNRS, Astroparticule et Cosmologie, F-75013 Paris, France.
[5]IFIC - Instituto de Física Corpuscular (CSIC - Universitat de València), c/Catedrático José Beltrán, 2, 46980 Paterna, Valencia, Spain.
[6]INFN, Sezione di Napoli, Complesso Universitario di Monte S. Angelo, Via Cintia ed. G, Napoli, 80126 Italy.
[7]Università di Napoli "Federico II", Dip. Scienze Fisiche "E. Pancini", Complesso Universitario di Monte S. Angelo, Via Cintia ed. G, Napoli, 80126 Italy.
[8]INFN, Sezione di Roma, Piazzale Aldo Moro 2, Roma, 00185 Italy.
[9]Universitat Politècnica de Catalunya, Laboratori d'Aplicacions Bioacústiques, Centre Tecnològic de Vilanova i la Geltrú, Avda. Rambla Exposició, s/n, Vilanova i la Geltrú, 08800 Spain.
[10]NCSR Demokritos, Institute of Nuclear and Particle Physics, Ag. Paraskevi Attikis, Athens, 15310 Greece.
[11]INFN, Sezione di Genova, Via Dodecaneso 33, Genova, 16146 Italy.
[12]University of Granada, Dept. of Computer Architecture and Technology/CITIC, 18071 Granada, Spain.
[13]Friedrich-Alexander-Universität Erlangen-Nürnberg, Erlangen Centre for Astroparticle Physics, Erwin-Rommel-Straße 1, 91058 Erlangen, Germany.
[14]Universitat Politècnica de València, Instituto de Investigación para la Gestión Integrada de las Zonas Costeras, C/ Paranimf, 1, Gandia, 46730 Spain.
[15]Nikhef, National Institute for Subatomic Physics, PO Box 41882, Amsterdam, 1009 DB Netherlands.
[16]University Mohammed V in Rabat, Faculty of Sciences, 4 av. Ibn Battouta, B.P. 1014, R.P. 10000 Rabat, Morocco.
[17]INFN, Sezione di Bologna, v.le C. Berti-Pichat, 6/2, Bologna, 40127 Italy.

[1]also at Dipartimento di Fisica, INFN Sezione di Padova and Università di Padova, I-35131, Padova, Italy

[18]Università di Bologna, Dipartimento di Fisica e Astronomia, v.le C. Berti-Pichat, 6/2, Bologna, 40127 Italy.
[19]KVI-CART University of Groningen, Groningen, the Netherlands.
[20]INFN, Laboratori Nazionali del Sud, Via S. Sofia 62, Catania, 95123 Italy.
[21]North-West University, Centre for Space Research, Private Bag X6001, Potchefstroom, 2520 South Africa.
[22]Instituto Español de Oceanografía, Unidad Mixta IEO-UPV, C/ Paranimf, 1, Gandia, 46730 Spain.
[23]University Mohammed I, Faculty of Sciences, BV Mohammed VI, B.P. 717, R.P. 60000 Oujda, Morocco.
[24]Subatech, IMT Atlantique, IN2P3-CNRS, Université de Nantes, 4 rue Alfred Kastler - La Chantrerie, Nantes, BP 20722 44307 France.
[25]Università di Salerno e INFN Gruppo Collegato di Salerno, Dipartimento di Matematica, Via Giovanni Paolo II 132, Fisciano, 84084 Italy.
[26]ISS, Atomistilor 409, Măgurele, RO-077125 Romania.
[27]University of Amsterdam, Institute of Physics/IHEF, PO Box 94216, Amsterdam, 1090 GE Netherlands.
[28]TNO, Technical Sciences, PO Box 155, Delft, 2600 AD Netherlands.
[29]Università degli Studi della Campania "Luigi Vanvitelli", Dipartimento di Matematica e Fisica, viale Lincoln 5, Caserta, 81100 Italy.
[30]Università La Sapienza, Dipartimento di Fisica, Piazzale Aldo Moro 2, Roma, 00185 Italy.
[31]Università di Bologna, Dipartimento di Ingegneria dell'Energia Elettrica e dell'Informazione "Guglielmo Marconi", Via dell'Università 50, Cesena, 47521 Italia.
[32]Cadi Ayyad University, Physics Department, Faculty of Science Semlalia, Av. My Abdellah, P.O.B. 2390, Marrakech, 40000 Morocco.
[33]University of the Witwatersrand, School of Physics, Private Bag 3, Johannesburg, Wits 2050 South Africa.
[34]Università di Catania, Dipartimento di Fisica e Astronomia "Ettore Majorana", Via Santa Sofia 64, Catania, 95123 Italy.
[35]INFN, LNF, Via Enrico Fermi, 40, Frascati, 00044 Italy.
[36]INFN, Sezione di Bari, via Orabona, 4, Bari, 70125 Italy.
[37]International Centre for Radio Astronomy Research, Curtin University, Bentley, WA 6102, Australia.
[38]University of Bari, Via Amendola 173, Bari, 70126 Italy.
[39]University Würzburg, Emil-Fischer-Straße 31, Würzburg, 97074 Germany.
[40]Western Sydney University, School of Computing, Engineering and Mathematics, Locked Bag 1797, Penrith, NSW 2751 Australia.
[41]Università di Salerno e INFN Gruppo Collegato di Salerno, Dipartimento di Fisica, Via Giovanni Paolo II 132, Fisciano, 84084 Italy.
[42]Università di Genova, Via Dodecaneso 33, Genova, 16146 Italy.
[43]Normandie Univ, ENSICAEN, UNICAEN, CNRS/IN2P3, LPC Caen, LPCCAEN, 6 boulevard Maréchal Juin, Caen, 14050 France.
[44]University of Granada, Dpto. de Física Teórica y del Cosmos & C.A.F.P.E., 18071 Granada, Spain.
[45]NIOZ (Royal Netherlands Institute for Sea Research), PO Box 59, Den Burg, Texel, 1790 AB, the Netherlands.
[46]Tbilisi State University, Department of Physics, 3, Chavchavadze Ave., Tbilisi, 0179 Georgia.
[47]Leiden University, Leiden Institute of Physics, PO Box 9504, Leiden, 2300 RA Netherlands.
[48]National Centre for Nuclear Research, 02-093 Warsaw, Poland.
[49]Institut Universitaire de France, 1 rue Descartes, Paris, 75005 France.
[50]University of Johannesburg, Department Physics, PO Box 524, Auckland Park, 2006 South Africa.
[51]Eberhard Karls Universität Tübingen, Institut für Astronomie und Astrophysik, Sand 1, Tübingen, 72076 Germany.
[52]Università di Pisa, Dipartimento di Fisica, Largo Bruno Pontecorvo 3, Pisa, 56127 Italy.
[53]Laboratoire Univers et Particules de Montpellier, Place Eugène Bataillon - CC 72, Montpellier Cédex 05, 34095 France.
[54]Friedrich-Alexander-Universität Erlangen-Nürnberg, Remeis Sternwarte, Sternwartstraße 7, 96049 Bamberg, Germany.
[55]Université de Haute Alsace, 68100 Mulhouse Cedex, France.
[56]University of Münster, Institut für Kernphysik, Wilhelm-Klemm-Str. 9, Münster, 48149 Germany.
[57]Utrecht University, Department of Physics and Astronomy, PO Box 80000, Utrecht, 3508 TA Netherlands.
[58]INFN, CNAF, v.le C. Berti-Pichat, 6/2, Bologna, 40127 Italy.